Real-time Inertia Estimation Via ARMAX Model Representation and Synchrophasor Measurements

Alexander Sanchez-Ocampo, *Student Member, IEEE*, Mario R. Arrieta Paternina, *Member, IEEE*, José Manuel Ramos-Guerrero, *Student Member, IEEE*, Gabriel E. Mejia-Ruiz, *Member, IEEE*, Juan M. Ramirez, *Member, IEEE*, Lucas Lugnani, *Member, IEEE*, Felix Munguia, *Student Member, IEEE*, Alejandro Zamora-Méndez, *Member, IEEE*, and Juan R. Rodriguez, *Member, IEEE*

***Abstract*—This paper introduces the real-time implementation with the actual hardware architecture environment (HAE) of an online estimation method that tracks the equivalent time-varying inertia in power systems. The proposed method enables automated and accurate inertia estimation, exploiting the ARMAX model representation and the Teager-Kaiser energy operator (TKEO) disturbance time detector. The effectiveness and high accuracy of the proposed framework are successfully validated in laboratory conditions with actual synchronized measurements from phasor measurement units (PMUs) over a real-time emulated New England 39-bus system. The estimate is achieved with a relative error ranging from 0.1% to 7%, even under noisy conditions and atypical measurement values. The literature reviewed does not report any estimation method that is more accurate than the one proposed in this work.**

Link to graphical and video abstracts, and to code: https://latamt.ieeer9.org/index.php/transactions/article/view/9594

***Index Terms*—Inertia estimation, Frequency response, PMU, Online estimation.**

I. Introduction

In traditional electrical systems, inertia is determined by the physical spinning mass of synchronous generators deployed on the electrical grid. In the event of a disturbance, the arrest of the frequency deviation of the power system relies on kinetic energy stored in the rotors of the generators. Hence, inertia plays a crucial role in the angular stability of the system during the disturbance [1].

The growing penetration of renewable energy sources (RESs) in modern power networks reduces the available inertia, increasing the frequency deviation, i.e. the Rate-of-Change-of-Frequency (RoCoF). Expanded deployment of RESs impacts the critical low-frequency modes of the grid and results in the formation of low inertia zones [2], [3]. The low inertia available in the power system increases the risk of tripping protective devices; it also drives controllers into extreme operating conditions and affects the operation of sensitive loads [4].

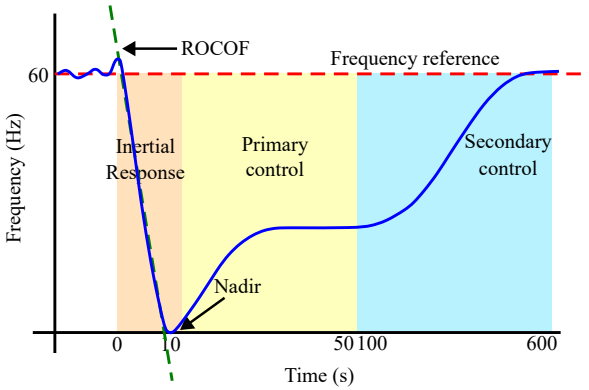

Fig. 1. Typical frequency behavior after power unbalance.

Fig. 1 depicts a typical frequency progression in a power system following a contingency. During the first few seconds, the power system's inertia influences the dynamic frequency behavior, i.e., the RoCoF.

The inertia of the electrical system is a time-varying parameter, making its real-time monitoring crucial for the timely execution of control actions [5]. Furthermore, under the current deregulated and uncertain environment, transmission system operators (TSOs) require accurate and real-time information on system inertia to make the appropriate decisions to ensure stability and increase the safety margins of the power network [6].

A. Literature Review

In recent years, extensive scientific efforts have been made to estimate the inertia of the power system. Still, several inertia estimators reported in the literature only work offline, based on the processing of data collected after an event [7]–[10]. Usually, these estimators are established on a simplified swing equation model and Phasor Measurement Unit (PMU) measurements [11]–[14]. Although this posterior estimation of inertia may be helpful in the planning stages of network operation, the information could arrive too late to take preventive or corrective real-time actions.

Online estimation algorithms have also been reported in [15]–[19]. These publications use PMU data, while some apply system identification approaches and stochastic models. Meanwhile, these iterative estimation algorithms based on the linearized swing equation represent an advance over offline estimators. These methods must be applied after a disturbance, and they require a disturbance detection mechanism to increase the accuracy of the inertia estimation [20], [21]. Some approaches for identifying

The associate editor coordinating the review of this manuscript and approving it for publication was José Miguel Sosa (*Corresponding author: Alejandro Zamora-Mendez*).

Alejandro Zamora-Méndez is with the Electrical Engineering Faculty, at the Michoacan University of Saint Nicholas of Hidalgo, Morelia, Michoacan, México (e-mail: azamoram@umich.mx).

A. Sanchez-Ocampo, and J. M. Ramirez are with the Center for Research and Advanced Studies of the National Polytechnic Institute, Guadalajara, México (e-mail: alexander.sanchez@cinvestav.mx, and joramirez@cinvestav.mx).

M. R. A. Paternina, J. Rodriguez, J. Guerrero, and F. Munguia are with the National Autonomous University of Mexico, México City, México, (e-mails: mra.paternina@fi-b.unam.mx, jr_rodriguez@fi-b.unam.mx, josema95@comunidad.unam.mx, and mupefe@ier.unam.mx).

G. E. Mejia-Ruiz is with the School of Electrical and Electronic Engineering at the Universidad del Valle, Cali, Colombia (e-mail: gabriel.mejia.ruiz@correounivalle.edu.co).

L. Lugnani is with the Department of Electrical Engineering at the University of Campinas, Campinas, Brazil (e-mail: llugnani@unicamp.br).

disturbance detection time are reported in [21] and [22]. Using a detrended fluctuation analysis (DFA) strategy. The first approach analyses a sliding data window. The perturbation time is established if the variation exceeds a threshold. The second solution employs the second derivative of frequency data (SDFD) with a data filter to remove measurement noise. This technique uses a small time scale to continually compute the RoCoF and SDFD; both parameters are analyzed, and the instant disruption can be identified. In summary, the first strategy requires many samples to detect the disturbance, whereas the second demands high complexity due to the computation of derivatives; notice that this is sensitive to how frequency is calculated, i.e. false spikes in frequency due to computation by angle derivative. On the other hand, the approach suggested in this investigation has low computing costs and small memory storage needs, resulting in timely and quick results.

Open research has indicated estimation errors near 5%, like [23], and [24], to support the current findings, whereas the error computed using the suggested technique is as low as 0.1%. This outcome emphasizes the relevance of this work.

Phasor measurement units (PMU) measurements are commonly exploited to estimate inertia values in online applications [25]–[28]. In [5], an expression relating the impedance and the transfer function of the system's frequency response to the injection of minor disturbances is derived to estimate the nodal inertia. A method of estimating inertia from ambient measurements of frequency and active power during regular system operation is presented in [29]. This method is based on applying the ARMAX model as a system identification method to the measurements and extracting the inertia values from the identified models, performing the estimation on a time scale of minutes or tens of minutes. In [30], a robust Kalman filter-based approach is proposed to analyze the generator inertia based on the discrete-time oscillation equation and synchrophasor measurements. In [16], the combination of deterministic and stochastic methods through an autoregressive (AR) model is presented for estimating inertia in the Italian power system. The application of a recursive least squares (RLS) fitted model, whose initial model is calculated from the non-recursive system identification method, is reported in [18]. A technique comparable to the one given in this study is outlined in [23], which employed N4SID as a system identification technique to get a swing equation model to estimate inertia after a disruption, and it is developed to be an online application. The methodology described in this current work is designed for real-time situations and enhances estimating errors.

In [6], a strategy for real-time estimation of the inertia constant of a power system is proposed based on a first-order nonlinear model in combination with the dynamic regressor and mixing (DREM) approach. Another real-time methodology is described in [31]. A machine learning model, including inertia, is developed to predict the system frequency response in real-time. This study used PMU measurements to approximate a swing equation model from estimating signal parameters via the rotational invariance techniques (ESPRIT) approach. Similarly, a real-time machine learning model for predicting nadir variation related to grid frequency support is performed in [3]. This methodology uses real-time inertia estimation using PMU measurements of synchronous devices to feed an adaptive PV frequency control strategy. This work trains a multivariate regression model for system inertia estimation.

The most recent work on real-time inertia estimation was developed in [32]. It used the Dynamic Mode Decomposition (DMD) approach to extract linear patterns to rebuild the swing equation and estimate the inertia parameter of a system area through PMU measurements. This work is focused on non-synchronous devices and estimates the time-varying inertia. For this reason, it does not implement time-detection strategies. These works in the real-time field report estimation errors are more significant than 1.5%. Therefore, this paper introduces better results related to estimation errors.

TABLE I
COMPARISON
AMONG DIFFERENT WORKS FOR INERTIA ESTIMATION

Ref.	Year	Swing equation	Sliding window	System identif.	PMUs	Online	Real time
[4]	2022	X					
[6]	2019			X	X		X
[7]	2020					X	
[8]	2022		X				
[9]	2022		X				
[10]	2022				X		
[11]	2019	X			X		
[12]	2019	X					
[13]	2021	X		X			
[14]	2020	X		X	X	X	
[15]	2022				X	X	
[16]	2020			X	X	X	
[17]	2020				X	X	
[18]	2021			X	X	X	
[19]	2022				X	X	
[23]	2020	X	X	X	X	X	
[25]	2022			X	X	X	
[26]	2022				X	X	
[27]	2022				X	X	
[28]	2022				X	X	
[31]	2020	X			X	X	X
[3]	2021				X	X	X
[32]	2024	X			X	X	X
Prop.		X	X	X	X	X	X

An extensive comparison among several inertia estimation algorithms is shown in Table I.

B. Problem Statement

Numerous research efforts are currently focusing on inertia performance in light of the significant need for solutions to improve inertial behavior. From this perspective, inertia estimate is viewed as one of the essential issues that power system operators will confront in the future because the displacement of rotational generation provokes a reduction in system inertia, which significantly impacts the stability and reliability of power grids [33]. Besides, the inertia reductions may cause significant RoCoF variations that may reach unacceptable levels after power imbalances, leading to large frequency deviations, cascading effects, or blackouts. As a result, operation centers must have mechanisms for real-time monitoring of the network's status to compute and predict the maximum frequency fluctuation. Although numerous studies have been conducted to estimate inertia in power systems, only some have been tested in actual conditions [3], [31].

C. Contribution

This paper proposes an efficient method to achieve real-time inertia estimation while addressing the above issues by exploiting the low-order ARMAX model for online analysis of the inertia of one or several rotating machines based on active power and frequency measurements. These data can be easily obtained using PMUs.

In summary, the approach for implementing this strategy is based on assessing the a generator bus's active power and frequency utilizing a hardware architecture environment (HAE). The frequency signal is monitored in real-time using the TKEO to detect when a disturbance occurs. Once a disruption occurs, the ARMAX algorithm generates a low-order transfer function

to approximate the swing equation of the generator. The inertia constant may thus be estimated via transfer function analysis.

Accordingly, the most significant contributions of this work are summarized as follows:

1) **Real-world implementation**: the inertia estimation has been validated using real-time simulations and real-world measurement data under noisy conditions. It is based on synchrophasor measurements, ensuring seamless integration into power systems without disrupting operations.
2) **Low computing costs**: precise disturbance time detection profits from the Teager-Kaiser energy operator for pinpointing the power imbalance, requiring only three samples (minimal memory storage) to improve the system's inertial response characterization.
3) **Estimation accuracy in the presence of noise**: the automated and accurate evaluation of the inertia, even under noisy conditions and atypical values, ensures reliable estimations with a relative error ranging from 0.1% to 7%.

The literature studied does not document any estimation approach that exceeds the accuracy of the method proposed in this study.

The remaining sections of the work are arranged as follows. In Section II, the theoretical foundations of the proposed method are detailed. Section III tests the estimator performance with real-time simulations under scenarios involving sudden generation reduction and load changes. Finally, concluding remarks are discussed in section IV.

II. Fundamentals

This section briefly overviews the mathematical foundation for estimating inertia in synchronous machines employing time-synchronized data via PMU. The PMU's frequency estimate is first addressed. The Teager-Kaiser energy operator for event detection and ARMAX modeling for inertia estimation are methodically specified, and the synchronous machine's inertia estimation is finally introduced.

A. Frequency Estimation by PMU Measurements

The measured signals, sinusoidal waveforms, through PMUs are given in the time domain, as follows [34]:

$$x(t)=X_m cos(\omega t+\phi) \tag{1}$$

The PMU estimates the frequency using the IEEE standard C37.118 [34]. Therefore, the PMU calculates the frequency from (1) by the following expression [34]:

$$f(t)=\frac{1}{2\pi}\frac{d\varphi(t)}{dt} \tag{2}$$

where $\varphi=\omega t+\phi$, $\omega=2\pi f$.

B. Disturbance Time Detection Via TKEO

The Teager-Kaiser energy operator (TKEO) carries the disturbance time detection. This operator is defined as a nonlinear energy operator for local (time) energy measure of oscillating signals, allowing to compute the energy of a real-valued signal $f(t)$, as follows [35]:

$$\Psi[\hat{f}(t)]=(\dot{\hat{f}}(t))^2-\hat{f}(t)\ddot{\hat{f}}(t) \tag{3}$$

where $\dot{\hat{f}}(t)$ and $\ddot{\hat{f}}(t)$ are the first and second derivatives of $\hat{f}(t)$, respectively.

In discrete time, the time derivatives are approximated by time differences defined by [35]

$$\Psi[f(n)]=f^2(n-1)-f(n-2)f(n). \tag{4}$$

Notice that only three samples are required for the energy estimation at each time instant. Then, a short window of samples is needed. For that, this instantaneous energy operator is ideal for local signal analysis with the ability to capture the signal energy fluctuations, allowing the proper detection of the disturbance instant [36].

The basic definition of the operator is straightforward and efficient, making the real-time implementation for an online estimation method plausible and able to track the equivalent time-varying inertia in power systems.

The straightforward implementation of the operator employs a frequency signal stemming from a PMU, as described by **Algorithm 1**. For this purpose, a 3-sample buffer is established to determine the correct disturbance instant (t_{dist}) subject to the threshold specified (tk_c) via actively monitoring frequency (f). According to our findings, this threshold is signal-dependent and related to the past observation and analysis of many disturbances thus, other users may be able to establish it using historical data.

C. ARMAX Modeling for Inertia Estimation

Active power and frequency measurements can estimate the inertia using the ARMAX model identification method. A pseudocode of the algorithm is implemented in **Algorithm 2**.

Online active power and frequency signals are processed with a disjoint window created from the time detected disturbance (t_{dist}). These signals, (ΔPe_{raw}) as an input signal and (Δf_{raw}) as an output signal, and (n_a,n_b,n_c,n_k) as coefficients related to the order of the system to be identified, the ARMAX model is estimated in the discrete form $G(z)$ (line 3 of **Algorithm 2**), as in [14], and then converted to continuous form $G(s)$ using bi-linear Tustin transformation with the *d2c* MATLAB function (line 4 of **Algorithm 2**).

D. Inertia Estimation

The inertia constant of a synchronous machine is directly attributed to the natural tendency of the rotor to oppose any action that attempts to change its momentum.

During a disturbance, energy must be redistributed to balance generation and load. The nominal inertia of a rotating machine is determined by its moment of inertia and rotational speed.

Algorithm 1 Disturbance real time detection via the Teager-Kaiser energy operator

Require: A frequency signal (f) is analysed in real time by taking samples around $f(n)$ at the n-th sample current time. The energy variation accepted tk_c.
Ensure: $n \geq 3$. ▷ Where n is the number of samples.
1: The frequency samples around the current time $t(n)$ are defined as $f(n)$,$f(n-1)$,$f(n-2)$.
2: Compute the real-time energy of f via (4).
3: **if** $\Psi[f(n)] > tk_c$ **then**
4: $t_{dist}=t(n)$; ▷ Where t is the time vector.
5: **end if**
return t_{dist}

Algorithm 2 ARMAX model for inertia estimation.

1: **Input:** [$\Delta Pe_{raw}(k)$; $\Delta f_{raw}(k)$, $k=t_0,...T$]; [n_a , n_b, n_c, n_k]
2: **Output:** $G(s)$
3: **Model estimation:** $G(z)$ = [A,B,C] = armax([Pe_{raw},f_{raw}],[n_a , n_b, n_c, n_k])
4: **Time transform:** $G(s)$ = d2c([A,B,C],'tustin')
return $G(s)$

At rated speed, it equals its kinetic energy E_{kin}, in megawatt seconds (MWs).

Therefore, the rotational kinetic energy is described as [37]:

$$E_{kin} = \frac{1}{2} J\omega^2 \tag{5}$$

where the machine's synchronous speed is denoted by ω, while the moment of inertia of its rotor is represented by J.

The inertia constant is the quantity of inertia per rated apparent power to calculate the inertia of a spinning rotor. The inertia constant of a single machine is stated as follows [37]:

$$H = \frac{J\omega^2}{2S_B} \tag{6}$$

where ω is 377 rad/s, H is the inertia constant that defines the link between the kinetic energy of the generator's rotors and the rated power S (in MVA) of synchronous machines, and S_B indicates the machine's base power in MVA.

In terms of the active power balance, (5) can be used to [37]:

$$2H\frac{d\Delta\omega}{dt} = \Delta P_m(t) - \Delta P_e(t) - D\Delta\omega \tag{7}$$

Or equivalently in terms of frequency, within $\omega = 2\pi f$

$$2H(2\pi)\frac{d\Delta f(t)}{dt} = \Delta P_m(t) - \Delta P_e(t) - (2\pi)D\Delta f \tag{8}$$

where $\Delta f(t)$, $\Delta Pe(t)$, $\Delta Pm(t)$ represent the frequency, active power, and mechanical power deviation in the time domain, respectively, and D is the load-damping constant.

Note that the expression (2π) is neglected in the following formulations since all variables are assumed to be in p.u. Mechanical power is also thought not to change rapidly when a power imbalance occurs. Thus, the oscillation equation (8) can be expressed in terms of inertia and frequency as [37]:

$$2H\frac{d\Delta f(t)}{dt} \approx -\Delta P_e(t) - D\Delta f \tag{9}$$

Applying the Laplace transform to obtain the transfer function of (9) after a perturbation, it is obtained the following relationship between the frequency deviation $\Delta F(s)$ and the active power deviation $\Delta Pe(s)$ [14]:

$$\frac{\Delta F(s)}{\Delta Pe(s)} = \frac{\frac{1}{2H}}{s + \frac{D}{2H}} \tag{10}$$

Now, H may be quantified in seconds and approximated online using the ARMAX model, utilizing the output $G(s)$ of **Algorithm 2**. The transfer function $G(s)$ describes the input-output relationship of the ARMAX model between (Δf_{raw}) and (ΔPe_{raw}), and is given by [14]:

$$G(s) = \frac{\Delta F_{raw}(s)}{\Delta Pe_{raw}(s)} \tag{11}$$

where $\Delta F_{raw}(s)$ and $\Delta Pe_{raw}(s)$ represent the frequency (output) and active power (input) deviation in the Laplace domain, respectively.

$G(s)$ obtained from the ARMAX algorithm is a second-order transfer function. It is necessary to apply an order reduction of $G(s)$ to compare it with (10) to attain a new first-order transfer function $G'(s)$ [14]:

$$G'(s) = \frac{\Delta F_{raw}(s)}{\Delta Pe_{raw}(s)} = \frac{\beta_0}{s + \alpha_0} \tag{12}$$

By inspection (10) and (12), the relationship $\hat{H} \approx -\frac{1}{2\beta_0}$ can be established.

III. Real-time Implementation

This section describes the laboratory-implemented system and test scenarios were deployed to evaluate and validate the performance of the proposed method in a real-time simulation environment.

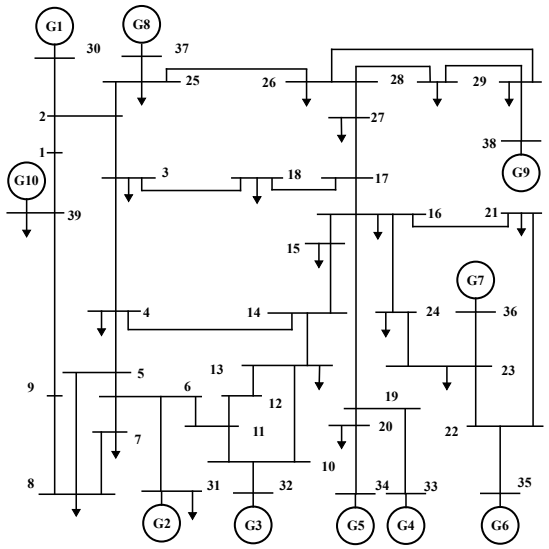

Fig. 2. Single-line diagram of the New England system.

A. Experimental Testbed

A case study is conducted on the New England system to investigate the feasibility of the proposed approach, whose one-line diagram is illustrated in Fig. 2. The power system is equipped with 19 loads, 10 machines, 39 buses, and 46 transmission lines. Poorly damped inter-area oscillation modes characterize these test systems and are widely used to study stability enhancement applications. Detailed parameters and operating conditions are given in [38].

The New England network was fully emulated on the dSPACE MicroLabBox platform and modeled in a Matlab & Simulink™ environment. The dSPACE emulator allows for real-time simulation of the transmission power grid with actual HAE. This unit has over 100 input/output channels, a 2 GHz dual-core processor, user-programmable FPGA, Ethernet communication channels, and low-voltage analogue output interfaces. The implementation scheme is illustrated in Fig. 3 later in this paper.

Synchrophasor measurements are performed with the SEL-351 device. This device performs synchronized, real-time measurements of voltages and currents, which comply with the IEEE standard C37.118-2005. This standard defines synchronized phasor measurements in power system applications, which allows any Intelligent Electronic Device (IED) that complies with this standard to communicate with each other. The SEL-351 relay connects via TCP/IP to a local area network (LAN) where the other test devices are connected to configure it; the relay web interface and Telnet protocol are used. Since this work, only needs synchrophasor measurements from a single IED, protocols such as DNP3 and IEC 61850, which have additional features to the C37.118-2005 standard, are not considered.

The phasor measurement data is transmitted from the PMU to the local computer via the IEEE C37.118-2005 [34] standard protocol. The disturbance detection and inertia estimation algorithms are then executed on the local computer. A Matlab script, described in **Algorithm 3**, implements algorithms that enable decoding the data frame transmitted by the PMU. The computer system's characteristics are a 2.1 GHz AMD Ryzer 5 processor, 20 GB of RAM, and a 64-bit WIN10 operating system.

The pseudocode of **Algorithm 3** uses a Matlab script to establish a TCP/IP connection; the PMU setup information is requested. This information allows data frames to be decoded from the

Algorithm 3 Get PMU synchrophasor data

INPUT: pmu_ip, pmu_port, pmu_idcode
OUTPUT: PMU synchrophasor data

```
function decodeDataFrame(raw_df, cfg2_data)
    for phasor in PHASORS do
        PHmag = phasor[0:4]
        PHang = radToDeg(phasor[4:8])
    end for
  return data_frame
Open: TCP/IP client socket
With pmu_ip, pmu_port, pmu_idcode connect to PMU
Send: command_frame asking for configuration frame 2
Receive: Raw configuration frame 2
Decode: Received raw configuration frame 2
Save: PMU info to configuration variable cfg2_data
Send: command_frame to turn on data transmission
loop
    if data_is_available_to_read, then
        Receive: Raw data frame
        Decode: data_frame = decodeDataFrame(raw_df, cfg2_data)
        if data_frame.CHK == getCRC(raw_data_frame) then
            data_error_flag = False
            Get: Synchrophasor data
        else
            data_error_flag = True
        end if
    end if
end loop
```

PMU. To read PMU measurement data, a tcpclient object is created to connect to a remote host (PMU). In this step, the IP address of the PMU and the port are needed. Then, byte by byte, a command frame asking for the configuration frame is formed. The most important fields in this command frame are the IDCODE field, which is a number that identifies the PMU, and the command field, which instructs the PMU to send the configuration frame. Once the configuration frame is received, the information necessary to decode the data frame, such as data format, number of phasors, number of analogue values, number of digital values, and conversion factor, is obtained. Following the order to initiate data transmission to the PMU, an endless loop is started to see if a data frame is received. When the algorithm gets a data frame, it begins by decoding the frame size field (number of bytes in the data frame) and splitting it into predetermined data chunks. Each data chunk is assigned a field with a byte size determined by IEEE C37.118-2005. These fields hold the PMU measurement data in a matching MATLAB variable. This procedure is continued until the script's execution is manually terminated.

The flowchart in Fig. 3 illustrates the algorithms employed in the proposed inertia estimation methodology. This comprehensive documentation encompasses every step deriving the inertia parameter from PMU measurements.

- **Hardware architecture**: This part contains the hardware architecture environment where the New England system is previously simulated in Simulink and then compiled in the dSPACE LabBox. It allows the extraction of a generator's three-phase voltage and current to be measured in real-time by the PMU, using the synchrophasor measurement and a satellite time stamp. This data is stored in a PDC (Phasor Data Concentrator).

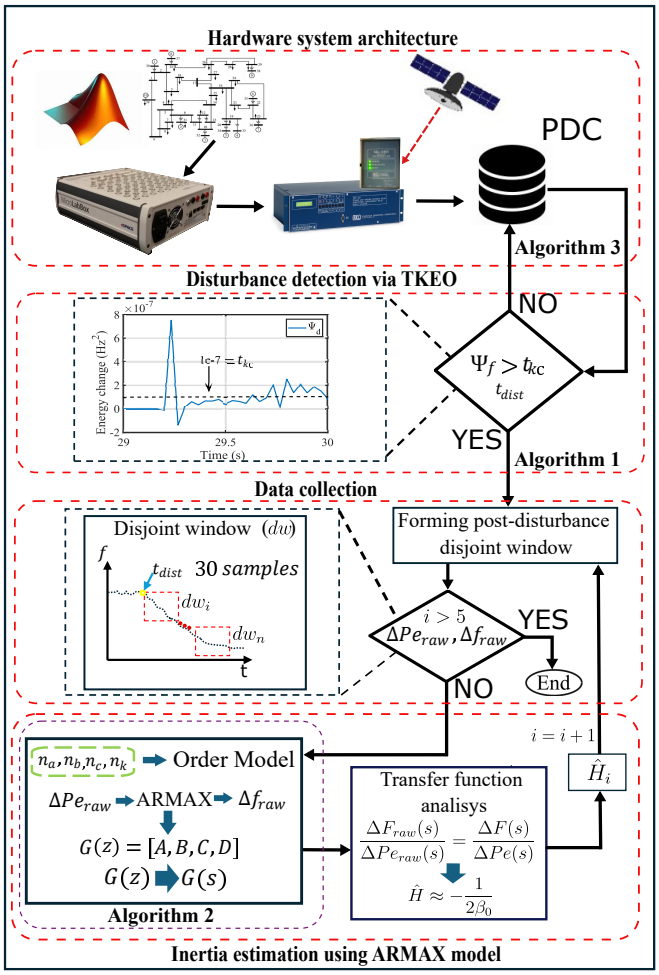

Fig. 3. Real-time simulation architecture.

- **Disturbance detection**: This phase relates to event identification by TKEO. In this step, the frequency energy signal Ψ_f, from PDC, is tracked in real-time to detect the time of disruption t_{dis} after a threshold t_{kc} is overrun.
- **Data collection**: The sampling windows are organized from t_{dis}, each corresponding to a measurement period (30 samples), i.e., the disjoint windows (dw_i) are constructed for 30 different samples until the desired estimation tests are achieved. The active power (Pe_{raw}) and frequency (f_{raw}) signals are collected for each sampling period.
- **Inertia estimation**: The active power and frequency signals feed the system identification technique. An identified linear system in discrete time $G(z)$ is obtained using the ARMAX method. The model is transformed into a continuous-time $G(s)$ to subsequently estimate the inertia parameter $\hat{H}_i$.

The oscillation equation enables analyzing the dynamic performance of the power system in a short period after the disturbance. This work considers 5 disjoint windows in the inertia estimation process, as shown in the data collection step in Fig. 3. The complete code for estimating inertia through PMU measurements is available at [39].

The physical connections and the laboratory prototype implemented are shown in Figs. 4 and 5, respectively.

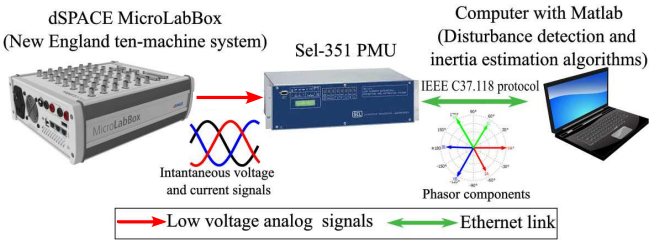

Fig. 4. Physical connections of the hardware used in the test bench.

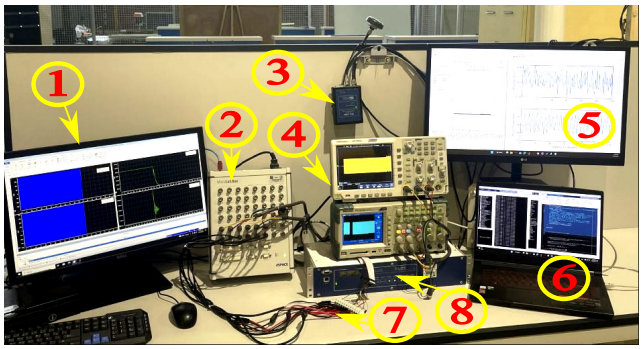

Fig. 5. Experimental testbed. (1) Human-machine interface of the transmission grid. (2) dSPACE MicroLabBox. (3) PMU GPS antenna. (4) Oscilloscopes. (5) Human-machine interface of the disturbance detector and inertia estimator. (6) Laptop with Matlab software. (7) Interface cables between the PMU and the dSPACE. (8) SEL-351 PMU.

B. Test Scenario

The efficiency and performance of the disturbance detection mechanism and inertia estimation algorithm are evaluated in response to a sudden load change at bus 16. PMU measurements are performed at bus 39, and electrical noise of between 10 dB and 20 dB is added to the measured current signals to verify the robustness of the proposed estimation method in a laboratory experimental environment. This experiment employs signals generated in simulation with MATLAB and using the Simulink environment. These signals emulate the measurements and the added noise is matched to the measurement noise of the current and potential transformers. These measurements are then obtained through dSPACE LabBox, which gives them a real-time connotation. Subsequently, the signals are acquired through a PMU 351-A and analyzed and processed at a remote station where the inertia estimation algorithm is implemented.

C. Results

Suitable operation of the inertia estimation algorithm involves timely and accurate recognition of the load change disturbance. The TKEO method indicates the instant at which the energy magnitude of the analyzed frequency signal changes, specifying the time instant at which the power imbalance starts.

The results of applying the TKEO method executing **Algorithm 1** are depicted in Fig. 6. This algorithm computes the energy within the detected frequency at G1 when the load change occurs at bus 16, as shown in Fig. 2. In this work, the threshold for tk_c is set at 1×10^{-7} Hz^2, to prevent false triggers caused by noise in the measured frequency signal. Under these conditions, the disturbance is detected via the TKEO method at $t_0 = 29.2$ s, giving the trigger signal for the start of the execution of the proposal's inertia estimation algorithm.

The computed active power, the measured frequency, and the estimated inertia are shown in Figs. 7 to 10. In these experiments, noise ranging from 0 to 20 dB was added to the voltage and current channels sensed by the PMU installed at generator G1. The active power is calculated based on the detected signals. The ARMAX technique is applied for inertia estimations using 30-sample windows.

The estimated active power, frequency, and inertia are depicted in Fig. 7. In this case, no noise is added, resulting in a relative error of 0.87%, as is shown in Table II.

Fig. 8 considers a noise measurement of 10 dB, the experiment with the slightest noise. This example shows a noisy, active power signal with a relative error of 0.51% (Table II), the closest approximation to the reference value.

Fig. 9 exhibits an average noise level (15 dB). It indicates an estimating error of 0.87% (Table II) in the most exact estimate. On the other side, Fig. 10 illustrates a high noise measurement level connected to the different test cases in this work. In this instance, the stated relative error from the nearest estimate is 0.07%.

To illustrate the noisy signals processed in this study, Fig. 11 depicts voltage signals with additional noise between 10 dB and 20 dB measured through PMU.

When the load change occurs, the active power increases from 6.5 pu to 7.5 pu. Under these power imbalance conditions, the measured frequency is reduced from its rated value (60 Hz) to 59.55 Hz, reaching its steady state 15 s after the disturbance occurs. The inertia estimations via the ARMAX method are very close to the rated value of 42 s in all experiments. It is important to note that noise in the signals can introduce random fluctuations, potentially affecting the accuracy or precision of the measurements. However, the inertia estimation error remains below 7%, evidencing that the implemented methodology is robust for noise levels up to 20 dB, as is shown in Table II.

D. Performance assessment

When the noise is included, the closest estimated result is 41.97 s, resulting in an estimated error of less than 1% in comparison with other online applications, Table III, that report an estimated error of greater than 1.5%. The current results are an acceptable approximation of the machine's inertia. As seen in Fig. 10(c), as the noisiest signal, coupled with the information set out in Table II, the inertia estimation approach effectively works when applied to signals with measurement noise.

Regarding the added noise to the signals, as seen in Fig. 8, which is the noisiest signal at 10 dB, coupled with the information given in Table II, it should be noted that the inertia estimation approach works effectively when noise is applied to the signals. Also, observing the information illustrated in Fig.11, where the highest signal-to-noise ratio (SNR) corresponds to 20 dB, it is useful to emphasize as the SNR improves, thus the signal

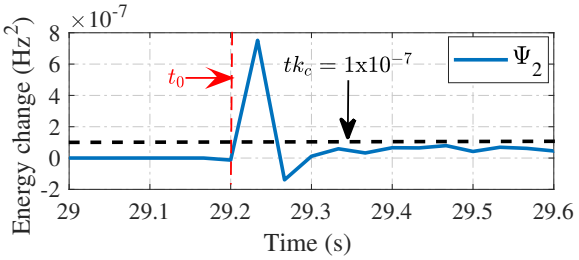

Fig. 6. Energy change of the frequency signal measured at G1.

TABLE II
RELATIVE ERROR OF EACH NOISE CASE

		Signal-to-noise ratio (SNR)							
		10 dB		15 dB		20 dB		Without noise	
Window	$H_{ref}(s)$	$H_{G1}(s)$	Relative error (%)	$H_{G1}(s)$	Relative error (%)	$H_{G1}(s)$	Relative error (%)	$H_{G1}(s)$	Relative error (%)
1		43.19	2.83	42.37	0.87	42.46	1.10	44.15	5.12
2		41.79	0.51	43.64	3.90	41.97	0.07	42.36	0.87
3	42	41.67	0.79	42.50	1.18	42.04	0.10	42.68	1.62
4		40.02	4.72	43.75	4.17	42.07	0.18	41.47	1.27
5		38.91	7.36	44.10	4.99	40.53	3.50	43.19	2.82

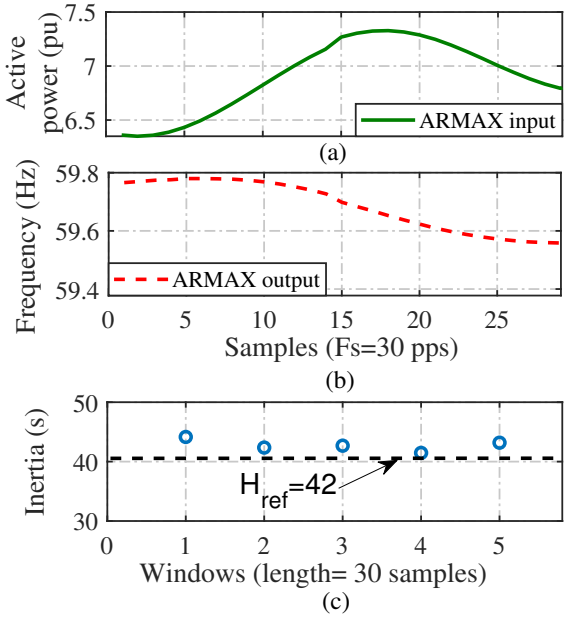

Fig. 7. Inertia estimation of generator G1 via ARMAX implemented in real-time.

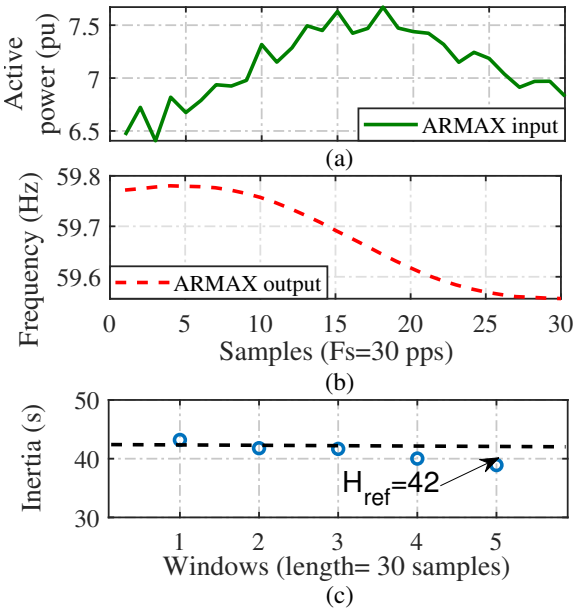

Fig. 8. Inertia estimation of generator G1 via ARMAX implemented in real-time, adding noise of 10 dB.

quality improves. Notice that the estimation error in Table II is significantly lower as the SNR increases, for instance, the relative

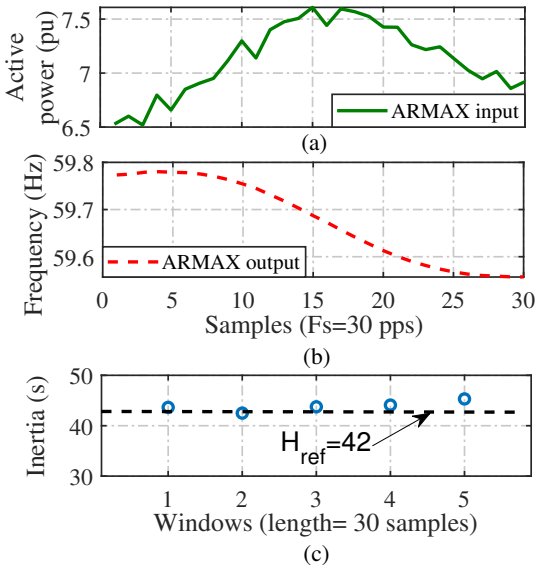

Fig. 9. Inertia estimation of generator G1 via ARMAX implemented in real-time, adding noise of 15 dB.

error is 7.36% for the fifth window at 10 dB and 3.5% at 20 dB.

On the other hand, when the signal contains higher noise levels, as shown in Fig.12 (a), which displays inertia estimates from

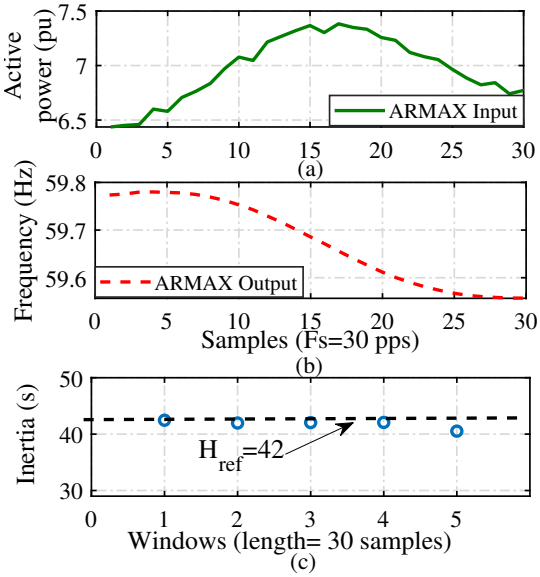

Fig. 10. Inertia estimation of generator G1 via ARMAX implemented in real-time, adding noise of 20 dB.

TABLE III
ERROR COMPARISON

Ref	Year	Measurement acquisition	Experimental noise	Error reported
[23]	2020	PMU	Measurement noise	$\leq 5\%$
[24]	2020	PMU	Measurement noise	$\leq 5\%$
[40]	2021	PMU	Measurement noise Ornstein-Uhlenbeck process	x
[32]	2024	PMU	Filter used to isolate noise	$\leq 2\%$
Prop.		PMU	Measurement noise plus 10, 15 and 20 dB	$\leq 1\%$

5 dB to 20 dB noise levels. As the SNR increases, the inertia estimate converges with the reference value, suggesting a higher estimation accuracy when the signal has less noise contamination.

For higher noise levels, such as 5 dB, which is considered a high noise level, the estimation error is maintained at low levels, as depicted in Fig.12 (b), exhibiting the relative estimation error for different SNR levels. It can be seen that even in low SNR scenarios, the relative error remains below 7%, demonstrating the effectiveness of the method. This behavior can be attributed to the ability of the PMU to filter noise during the phasor estimation process, which contributes to the reliability of the results obtained and indicates a high accuracy of the method under noise conditions.

Regarding the results found in this work. Table III compares the outcomes of this investigation to those of comparable real-time inertia estimation methods. This comparison seeks to uncover extra information on the sensor utilized in other strategies and the noise treatment in each scheme. The goal is to have a reasonable foundation to compare the outcomes presented here as the most accurate compared to the existing study findings.

For instance, the outcomes reported in [23] and [24] are obtained by employing PMU measurements from real-word grids, which only involve noise from the measurements and use the raw data for the inertia estimation strategy. On the contrary, [32] engages noise filters to isolate and prevent the noise from the PMU measurements. On the other hand, [40] is robust against noise owing to the formulation for inertia estimation, which avoids numerical issues and filters spikes and noise.

IV. CONCLUSIONS

In this paper, we propose the implementation of a test bed for real-time emulation with HAE simulation to evaluate an online estimation method for the inertia constant of the power system. Firstly, the ARMAX system identification method is used to model a single input, single output black-box model to estimate the inertia from active power and frequency signals.

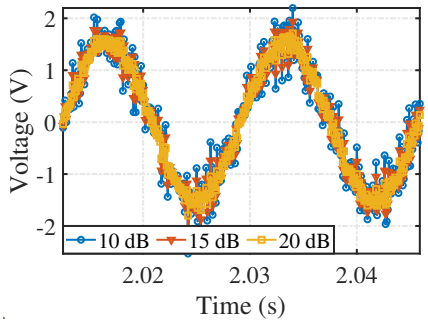

Fig. 11. Noise levels implemented on measured signals.

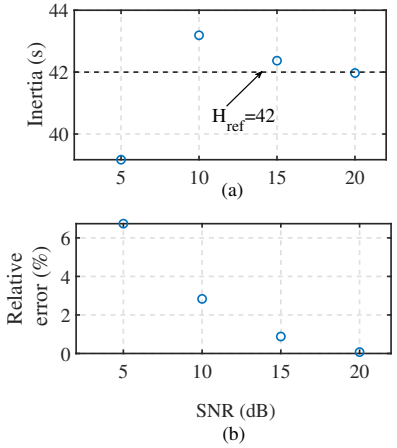

Fig. 12. Estimation error vs the SNR.

Then, the Teager-Kaiser energy operator method is exploited to determine when the load change disturbance starts accurately. The advantages of this method lie in having low computing costs and requiring minimal memory storage (only three samples to capture the signal energy fluctuations), making the real-time implementation of an online estimation method plausible.

The proposed method was tested on the 39-bus New England system. The results confirmed that the inertia constant of the power system (individual generator) is updated in real-time with an inaccurate range of 0.1% to 7% under electrical noise circumstances in the signal measurements. The results indicate that the proposed method allows updating the system inertia estimation in real-time and on a scale of seconds.

REFERENCES

[1] K. S. Ratnam, K. Palanisamy, and G. Yang, "Future low-inertia power systems: Requirements, issues, and solutions - a review," *Renewable and Sustainable Energy Reviews*, vol. 124, p. 109773, 2020, doi: https://doi.org/10.1016/j.rser.2020.109773.

[2] A. Fernández-Guillamón and et al, "Power systems with high renewable energy sources: A review of inertia and frequency control strategies over time," *Renewable and Sustainable Energy Reviews*, vol. 115, p. 109369, 2019, doi: https://doi.org/10.1016/j.rser.2019.109369.

[3] Y. Su and et al, "An adaptive pv frequency control strategy based on real-time inertia estimation," *IEEE Trans. Smart Grid*, vol. 12, no. 3, pp. 2355–2364, 2021, doi: 10.1109/TSG.2020.3045626.

[4] B. Wang and et al, "An improved electromechanical oscillation-based inertia estimation method," *IEEE Trans. Power Systems*, vol. 37, no. 3, pp. 2479–2482, 2022, doi: 10.1109/TPWRS.2022.3156441.

[5] W. Zhang and et al, "Impedance-based online estimation of nodal inertia and primary frequency regulation capability," *IEEE Trans. Power Systems*, vol. 38, no. 3, pp. 2748–2760, 2023, doi: 10.1109/TPWRS.2022.3186525.

[6] J. Schiffer, P. Aristidou, and R. Ortega, "Online estimation of power system inertia using dynamic regressor extension and mixing," *IEEE Trans. Power Systems*, vol. 34, no. 6, pp. 4993–5001, 2019, doi: 10.1109/TPWRS.2019.2915249.

[7] A. Gorbunov, A. Dymarsky, and J. Bialek, "Estimation of parameters of a dynamic generator model from modal PMU measurements," *IEEE Trans. Power Systems*, vol. 35, no. 1, pp. 53–62, 2020, doi: 10.1109/TPWRS.2019.2925127.

[8] D. Li and et al, "Area inertia estimation of power system containing wind power considering dispersion of frequency response based on measured area frequency," *IET Generation, Transmission & Distribution*, vol. 16, no. 22, pp. 4640–4651, 2022, doi: https://doi.org/10.1049/gtd2.12628.

[9] H. Yin and et al, "Precise rocof estimation algorithm for low inertia power grids," *Electric Power Systems Research*, vol. 209, p. 107968, 2022, doi: https://doi.org/10.1016/j.epsr.2022.107968.

[10] T. Kerdphol and et al, "Inertia estimation of the 60 hz japanese power system from synchrophasor measurements," *IEEE Trans. Power Systems*, pp. 1–1, 2022, doi: 10.1109/TPWRS.2022.3168037.

[11] G. Cai and et al, "Inertia estimation based on observed electromechanical oscillation response for power systems," *IEEE Trans. Power Systems*, vol. 34, no. 6, pp. 4291–4299, 2019, doi: 10.1109/TPWRS.2019.2914356.

[12] C. Phurailatpam and et al, "Measurement-based estimation of inertia in ac microgrids," *IEEE Trans. Sustainable Energy*, vol. 11, no. 3, pp. 1975–1984, 2019, doi: 10.1109/TSTE.2019.2948224.
[13] C. Phurailatpam, Z. H. Rather, B. Bahrani, and S. Doolla, "Estimation of non-synchronous inertia in ac microgrids," *IEEE Trans. Sustainable Energy*, vol. 12, no. 4, pp. 1903–1914, 2021, doi: 10.1109/TSTE.2021.3070678.
[14] L. Lugnani and et al, "Armax-based method for inertial constant estimation of generation units using synchrophasors," *Electric Power System Research*, vol. 180, p. 106097, 2020, doi: https://doi.org/10.1016/j.epsr.2019.106097.
[15] B. Wang and et al, "Online inertia estimation using electromechanical oscillation modal extracted from synchronized ambient data," *Journal of Modern Power Systems and Clean Energy*, vol. 10, no. 1, pp. 241–244, 2022, doi: 10.35833/MPCE.2020.000105.
[16] F. Allella and et al, "On-line estimation assessment of power systems inertia with high penetration of renewable generation," *IEEE Access*, vol. 8, pp. 62 689–62 697, 2020, doi: 10.1109/ACCESS.2020.2983877.
[17] D. Yang and et al, "Data-driven estimation of inertia for multi-area interconnected power systems using dynamic mode decomposition," *IEEE Trans. Industrial Informatics*, 2020, doi: 10.1109/TII.2020.2998074.
[18] P. Makolo, R. Zamora, and T.-T. Lie, "Online inertia estimation for power systems with high penetration of res using recursive parameters estimation," *IET Renewable Power Generation*, 2021, doi: https://doi.org/10.1049/rpg2.12181.
[19] B. Wang and et al, "Power system inertia estimation method based on maximum frequency deviation," *IET Renewable Power Generation*, vol. 16, no. 3, pp. 622–633, 2022, doi: https://doi.org/10.1049/rpg2.12367.
[20] P. Wall and V. Terzija, "Simultaneous estimation of the time of disturbance and inertia in power systems," *IEEE Trans. Power Del.*, vol. 29, no. 4, 2014, doi: 10.1109/TPWRD.2014.2306062.
[21] P. M. Ashton, C. S. Saunders, G. A. Taylor, A. M. Carter, and M. E. Bradley, "Inertia estimation of the GB power system using synchrophasor measurements," *IEEE Trans. on PS*, vol. 30, no. 2, 2015, doi: 10.1109/TPWRS.2014.2333776.
[22] W. Wang and et al, "Fast and accurate frequency response estimation for large power system disturbances using second derivative of frequency data," *IEEE Trans. Power Systems*, vol. 35, no. 3, pp. 2483–2486, 2020, doi: 10.1109/TPWRS.2020.2977504.
[23] F. Zeng and et al, "Online estimation of power system inertia constant under normal operating conditions," *IEEE Access*, vol. 8, pp. 101 426–101 436, 2020, doi: 10.1109/ACCESS.2020.2997728.
[24] Y. Cui, S. You, and Y. Liu, "Ambient synchrophasor measurement based system inertia estimation," in *2020 IEEE Power & Energy Society General Meeting (PESGM)*, 2020, pp. 1–5, doi: 10.1109/PESGM41954.2020.9281662.
[25] J. Liu and et al, "Online estimation of poi-level aggregated inertia considering frequency spatial correlation," *IEEE Trans. Power Systems*, pp. 1–13, 2022, doi: 10.1109/TPWRS.2022.3197129.
[26] B. Tan, J. Zhao, V. Terzija, and Y. Zhang, "Decentralized data-driven estimation of generator rotor speed and inertia constant based on adaptive unscented kalman filter," *Intern. J. of Electrical Power & Energy Systems*, vol. 137, p. 107853, 2022, doi: https://doi.org/10.1016/j.ijepes.2021.107853.
[27] J. Guo, X. Wang, and B.-T. Ooi, "Estimation of inertia for synchronous and non-synchronous generators based on ambient measurements," *IEEE Trans. Power Systems*, vol. 37, no. 5, pp. 3747–3757, 2022, doi: 10.1109/TPWRS.2021.3134818.
[28] ——, "Online purely data-driven estimation of inertia and center-of-inertia frequency for power systems with vsc-interfaced energy sources," *Intern. J. of Electrical Power & Energy Systems*, vol. 137, p. 107643, 2022, doi: https://doi.org/10.1016/j.ijepes.2021.107643.
[29] K. Tuttelberg and et al, "Estimation of power system inertia from ambient wide area measurements," *IEEE Trans. Power Systems*, vol. 33, no. 6, pp. 7249–7257, 2018, doi: 10.1109/TPWRS.2018.2843381.
[30] J. Zhao, Y. Tang, and V. Terzija, "Robust online estimation of power system center of inertia frequency," *IEEE Trans. Power Systems*, vol. 34, no. 1, pp. 821–825, 2019, doi: 10.1109/TPWRS.2018.2879782.
[31] R. K. Panda and et al, "Online estimation of system inertia in a power network utilizing synchrophasor measurements," *IEEE Trans. Power Systems*, vol. 35, no. 4, pp. 3122–3132, 2020, doi: 10.1109/TPWRS.2019.2958603.
[32] Y. Li and et al, "Real-time estimation of time-varying inertia for non-synchronous devices using streaming dynamic mode decomposition," *Intern. J. of Electrical Power & Energy Systems*, vol. 157, p. 109847, 2024, doi: https://doi.org/10.1016/j.ijepes.2024.109847.
[33] J. Zhao and et al, "Roles of dynamic state estimation in power system modeling, monitoring and operation," *IEEE Trans. Power Systems*, vol. 36, no. 3, pp. 2462–2472, 2021, ddoi: 10.1109/TPWRS.2020.3028047.
[34] "IEEE standard for synchrophasor measurements for power systems," *IEEE Std C37.118.1-2011 (Revision of IEEE Std C37.118-2005)*, pp. 1–61, 2011, doi: 10.1109/IEEESTD.2011.6111219.
[35] P. Maragos and A. Potamianos, "Higher order differential energy operators," *IEEE Signal Processing Letters*, vol. 2, no. 8, pp. 152–154, 1995, doi: 10.1109/97.404130.
[36] D. Rodales, , and et al., "Model-free inertia estimation in bulk power grids through o-splines," *Intern. J. of Electrical Power & Energy Systems*, vol. 153, p. 109323, 2023, doi: https://doi.org/10.1016/j.ijepes.2023.109323.
[37] P. Kundur, N. J. Balu, and M. G. Lauby, *Power system stability and control*. McGraw-hill New York, 1994, vol. 7.
[38] T. Athay, R. Podmore, and S. Virmani, "A practical method for the direct analysis of transient stability," *IEEE Trans. Power Apparatus and Systems*, vol. PAS-98, no. 2, pp. 573–584, 1979, doi: 10.1109/TPAS.1979.319407.
[39] A. Sanchez-Ocampo and et al, *Real-time inertia estimation*, 2024 (accessed Feb 27, 2024), https://github.com/Alo991/Real-time-inertia-estimation.git.
[40] M. Liu, J. Chen, and F. Milano, "On-line inertia estimation for synchronous and non-synchronous devices," *IEEE Transactions on Power Systems*, vol. 36, no. 3, pp. 2693–2701, 2021, doi: 10.1109/TPWRS.2020.3037265.

Alexander Sánchez Ocampo received his B.Eng. in Electrical Engineering from Pascual Bravo university institution, Colombia, in 2017, and his M.Sc. in Electrical Engineering from CINVESTAV, Mexico, in 2021. He is currently pursuing the Ph.D. degree in electrical engineering at CINVESTAV, Guadalajara, focusing on regional inertia estimation, and frequency monitoring.

Mario R. Arrieta Paternina (M' 11) holds a B.Eng. and M.Eng. in Electrical Engineering from National University of Colombia, Medellin, Colombia, in 2007 and 2009, respectively. In 2017, he obtained his D.Sc. degree in Electrical Engineering from CINVESTAV, and he joined the Department of Electrical Engineering at the UNAM.

José Manuel Ramos (Member, IEEE) received the B.Eng. and M.Eng. degrees in electrical power systems from the National Autonomous University of Mexico (UNAM) in 2022 and 2024, respectively. Since 2024, he has been working towards the Ph.D. degree in Electrical Engineering at UNAM. His areas of interest include the design of electrical machines, interconnection of renewable energy to the grid, and stability of power systems through modal patterns.

Gabriel Mejia-Ruiz holds a B.Eng. in Control Engineering from the National University of Colombia (2007) and an M.Eng. from the University of Antioquia (2015). In 2023, he obtained a Ph.D. in Electrical Engineering from the National Autonomous University of Mexico (UNAM). His expertise includes the design, modeling, and prototyping of grid-connected power electronic converters and real-time simulations of inverter-based power systems.

Juan M. Ramirez-Arredondo (Member, IEEE) received the Ph.D. degree in electrical engineering from UANL-Mexico, San Nicolás de los Garza, Mexico, in 1992.,He joined the Department of Electrical Engineering, CINVESTAV Guadalajara, Guadalajara, Mexico, in 1999, where he is currently a full-time Professor. His research interests include smartgrids, microgrids, and power electronics applications., Dr. Ramirez-Arredondo is also a member of the Mexican Research System.

Lucas Lugnani Fernandes holds a PhD in Electrical Engineering from State University of Campinas, UNICAMP, Brazil (UNICAMP). Graduated in Electrical Engineering from UTFPR (2016) and master's in electrical engineering from UNICAMP (2018). He has experience in Electrical Engineering Power Systems, with an emphasis on parameter estimation, frequency stability, angular stability and synchrophasors, control and Lyapunov theory. He is currently pursuing the Post-Doctorate in UNICAMP, Brazil.

Félix Ernesto Munguía Pérez holds a B. Eng. in Electronics and Telecommunications (2007), an M.Sc. in Instrumentation and Data Processing, both from Tecnólogico Nacional de México campus Culiacán (2016) and he is currently pursuing his D.Eng. in Renewable Energy from UNAM-IER. At this time, he is doing research on WAMCS at Universidad Michoacana de San Nicolás de Hidalgo.

Alejandro Zamora-Méndez (M' 11) obtained his B.S. and M.Sc. in Electrical Engineering from Universidad Michoacana de San Nicolas de Hidalgo (UMSNH), Morelia, Mexico, in 2005 and 2008, respectively. He joined the Electrical Engineering Faculty, UMSNH in 2008. He received a D.Sc. degree in Electrical Engineering from CINVESTAV-Guadalajara in 2016.

Juan R. Rodríguez-Rodríguez received the B.Eng. and Ph.D. degrees in electrical engineering from the Instituto Tecnológico de Morelia, Morelia, Mexico, in 2009 and 2015, respectively. He is currently Associate Professor in the Department of Electrical Energy at UNAM, Mexico. His current research interests include power electronics converters, smart-grids, and renewable energy.